5-2022

Multistage modeling of fatigue of Ti-6Al-4V fabricated by different additive manufacturing techniques

Lionardo Lado
University of Tennessee at Chattanooga, wxv819@mocs.utc.edu

Saeed Ataollahi
University of Tennessee at Chattanooga

Mohammad J. Mahtabi
University of Tennessee at Chattanooga

Multistage Modeling of Fatigue of Ti-6Al-4V Fabricated by Different Additive Manufacturing Techniques

Lionardo Lado*, Saeed Ataollahi*, and Mohammad J. Mahtabi*

Departmental Honors Thesis

*Department of Mechanical Engineering
The University of Tennessee at Chattanooga, Chattanooga, TN, 37403

Examination Date: 4/8/2022

Mohammad Mahtabi, Ph.D.
Assistant Professor of Mechanical Engineering
Thesis Director

Hamdy Ibrahim, Ph.D.
Assistant Professor of Mechanical Engineering
Department Examiner

Abstract

Thanks to its high strength-to-weight ratio and corrosion resistance, Ti-6Al-4V has gained a lot of attention in additive manufacturing (AM) of complex parts with aerospace and medical applications. The realistic loading condition in these applications is mostly cyclic. However, the main challenge with AM of this alloy - and in general AM of metallic parts - is fatigue resistance and durability of the part, which has been reported to be much lower than the conventional materials. In this study, fatigue life performance of three additive manufacturing methods was compared using the Multistage Fatigue model (MSF). MSF model predicts the fatigue life of a material by incorporating microstructural features and defects such as grain size, pore size and pores nearest neighbors. The studied AM methods include Laser Engineered Net Shaping (LENS), Electron Beam Melting (EBM), and Selective Laser Melting (SLM). Each of these processes uses a different method in constructing the three-dimensional object yielding different microstructure. For this work, microstructural data were collected from previous experimental studies. Scanned Electron Microscopy (SEM) images were used to examine the fracture surfaces of the AM specimens and the defects responsible for fatigue failure. MSF divides fatigue life into three stages of crack incubation, microstructurally small crack and long crack stages. With an emphasis on the microstructurally small crack growth and long crack growth, a comparison was performed after calibrating the parameters for each of the AM processes. The results showed the predicted fatigue life is consistent with experimental results. In addition, fatigue resistance governing parameters which were process dependent, were identified for all AM methods.

Keywords: Multistage fatigue, MSF, Additive Manufacturing, Ti-6Al-4V, EBM, LENS, SLM

1- Introduction

Additive manufacturing (AM) has shown a great potential in minimization of material waste and lowering the fabrication cost and labor of complex parts. It allows for the creation of customized three-dimensional items that can be functional. A significant amount of attention has been paid to this advanced manufacturing process in many industries, especially when it comes to fabrication from metallic alloys. Among metallic alloys that are widely used in AM, titanium alloys have a considerable share in the market. As a main titanium alloy, Ti-6Al-4V possesses unique properties such as combination of high strength, toughness, corrosion resistance, ductility and biocompatibility [1, 2]. These characteristics have made Ti-6Al-4V a perfect candidate for medical and aerospace applications [3, 4]. For instance, its corrosion resistance and biocompatibility make it a suitable option for producing surgical implants. Similar to additive manufacturing of other metals, the main challenge in using Ti-6Al-4V is to obtain equal or even better mechanical properties compared to wrought material. Due to large number of process parameters such as laser power, scanning speed, layer thickness, hatch spacing, etc., the microstructure of final product may vary significantly by alteration of each one of these process parameters. As a result, mechanical properties vary by different microstructure. In the current level of AM, we can generally obtain monotonic mechanical properties as good as wrought material. However, due to formation of various types of defects like pores, cracks and inclusions, and also lack of fusion between subsequent layers, fatigue resistance of AM materials is mostly inferior compared to their wrought counterparts. Although, post processing methods like heat treatment [5] and hot isostatic pressing (HIP) [6, 7] can reduce the number of defects, using HIP will reduce

the part accuracy and microstructure affected by heat treatment may not be consistent with the application of the final product. Moreover, post processing reduces the cost-effectiveness of AM. It has been reported that the morphology of the final microstructure in Ti-6Al-4V, varies depending on the implemented additive manufacturing method. The fact that Ti-6Al-4V is an $\alpha + \beta$ alloy, increases this variability. For instance, different morphology of equiaxed, columnar or acicular (which usually form in the martensitic phase [3, 8]) grains can be obtained using a certain AM process.

Employing predictive methods to study the fatigue behavior of additively manufactured Ti-6Al-4V can provide a better understanding on how each AM process yields a certain fatigue life. Multistage Fatigue (MSF) model is a microstructure-based powerful tool which originally was introduced for predicting fatigue life of the cast aluminum alloy [9]. It can explicitly incorporate the effect of different microstructural features and defects into the prediction of fatigue life. It has also been used to calibrate and then predict fatigue behavior of many wrought materials, and since it is a multiscale model that can get microstructural descriptor resulted from any material processing method, it can be used to develop a linkage for process-structure-property in AM of Ti-6Al-4V. In this study, by employing the multistage fatigue (MSF) model, the Ti-6Al-4V fabricated using different AM methods, are compared to determine the process dependent parameters in MSF. Fatigue life is divided into three stages in MSF modeling: crack incubation, microstructurally small crack (MSC) and long crack (LC). By changing parameters in equations of each stage, the model can be calibrated to each material. Here, the focus of this study is on the microstructurally small crack stage. It is because in as-built (considering that post processing can change microstructural features of AM material, the as-built Ti-6Al-4V fabricated using different AM methods is investigated) additively manufactured material, there are defects right after fabrication that are considered as stress risers. This will deem the incubation stage to have minor effect, and it is reasonable to mainly focus on the growth of a crack around a micro-notch and also the long crack growth stage. The studied AM methods include Laser Engineered Net Shaping (LENS), Electron Beam Melting (EBM), and Selective Laser Melting (SLM).

As part of efforts for predicting and tailoring the fatigue related characteristics of AM materials, this work considers Ti-6Al-4V as a case study to identify which parameters of the microstructurally small crack stage in the multistage fatigue model code, are process dependent. A common issue when using the MSF code for additively manufactured metals is that each process may affect the fatigue behavior of the material. This is due to the fact that when using the code, microstructural data heavily influence the effect each parameter will have on the fatigue performance of the material. Therefore, each considered additive manufacturing process will need to be calibrated in the MSF code while accounting for its sensitivity when adding the required data. The results of this study will not only increase efficiency for fatigue modeling of additively manufactured Ti-6Al-4V but can possibly be used alongside the MSF results of other AM materials to develop a unified fatigue prediction method for AM materials.

By adding microstructural data provided from the scanned electron microscopy to the MSF model code, we can create strain-controlled fatigue curves for each set of input data that is related to each of the AM methods. Even though it is the same material being fabricated, the three additive manufacturing methods can influence the values for the microstructural characteristics. These characteristics are microstructural features (grain size, orientation, etc.) and defects (pore size, spacing, porosity, etc.). Laser Engineered Net Shaping (LENS) fabricated Ti-6A-4V specimens has shown to have a unique microstructural feature in where the grains have a distinguished shape. When examined, the beta grains were columnar and there were fine alpha morphologies.

Depending on the power input, high magnification of the morphology can show a martensite microstructure with acicular alpha or mix of alpha-beta lamellae [3]. This is determined to be a result of multiple factors such as the cyclic heating, directional heat extraction and the fast-cooling rate [3]. The tensile fatigue testing for the Ti-6Al-4V was comparable to the conventional version of the material. However, the ductility of the LENS fabricated is lower and would need to be heat treated to be able to make a proper comparison of the material [10]. In addition, it was also determined that the porosity also can shorten the fatigue life of the specimen when it is not heat-treated. Electron Beam Melting (EBM) demonstrates a similar morphology to LENS in that its beta grains are columnar. However, during the fabrication process the specimens are slowly cooled, unlike LENS which needed to be fast cooled. The reason it needed to be slowly cooled was to decompose of any martensite phases during solidification [10]. Thus, it will result in an alpha-beta lamellae at high magnification [3] . Since EBM is a powder bed fusion technique, it will have two types of pores that can form during the built process. The first type is gas pore that is caused by trapped gas in the specimen and is spherical, while the other type is caused by insufficient melting. In fatigue testing of EBM fabricated Ti-6Al-4V, it demonstrates a high tensile strength when compared to heat treated Ti-6Al-4V. In addition, because of the lack of the martensite phase, the ductility of the EBM specimen is higher than that of the LENS [3]. Selective Laser Melting (SLM) exhibits similar microstructural morphologies to the other additive manufacturing methods. This is demonstrated in this method by having columnar beta grains, with acicular alpha martensite [11]. This will give the material a higher tensile strength, but it will suffer from lower ductility as proven also in the LENS method. Improving the ductility of the specimen to have alpha beta lamellae can only be done by using heat treatment or cyclic reheating during the build process [11] .

2- Materials and method

Data from previous experimental studies on Ti-6Al-4V using each AM method, were collected from literature. Three types of data were used for calibration of MSF model: (1) Fatigue-related graphs for comparison, (2) microstructural features and defects, (3) mechanical properties. All cyclic strain-controlled fatigue tests which were conducted under a load ratio of R = -1, were chosen since it was the most commonly used load ratio for fatigue of AM methods. The graphs used in this study are the strain amplitude versus number of cycles. For each method, the focus was on Ti-6Al-4V without any heat-treatment, referred to as as-built. The WebPlotDigitizer [12] is a tool used to extract underlying numerical data from graphs of the fatigue tests. Before the data was extracted, the exported graphs needed to be scaled properly in the plot digitizer, such as setting the graphs as semi-log. When completed, each datapoint on the graph was marked and the coordinates of them were downloaded in a file to be imported into the multistage fatigue code for calibration. Moreover, mechanical and microstructural data for each AM method needed to be collected. In cases where microstructural features (grain size, orientation, etc.) and defects (pore size, spacing, porosity, etc.) were not reported, an image processing software was used to quantify them. ImageJ software [13] was implemented for measuring the size and number of grains and voids in the SEM images. Figure 1 shows an example of void formation in Ti-6Al-4V fabricated by LENS methods which was quantified in this study. Some of the compiled data are summarized in Table 1. PORENND is an important parameter that is needed to produce the curve which is defined as pores nearest neighbors and implies the proximity of pores in a specimen.

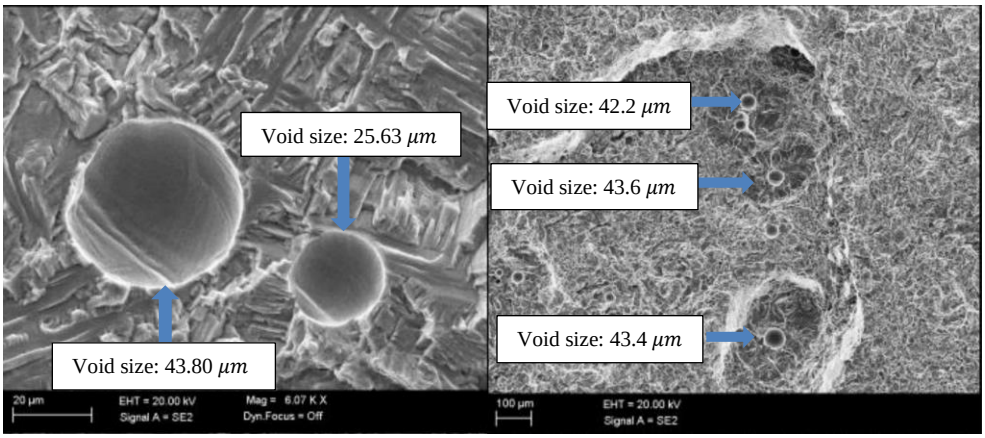

Figure 1- Void formation in Ti-6Al-4V fabricated using LENS method (These features were quantified for MSF model).

Table 1 - Microstructural parameters for the multistage fatigue model for Ti-6Al-4V

Parameter	**Conventional**	**EBM**	**LENS**	**SLM**
Pore size (µm)	0.001	73	42.86	22
PoreNND (µm)	0.00708	513	303.6	409.47
Grain size (µm)	5	4.68	320.4	2.89

The multistage fatigue code which was originally developed by McDowell et al. [9], is a microstructure-sensitive simulation tool for fatigue modeling. The code characterizes fatigue life into three stages. The first stage is the crack incubation, which is the number of cycles needed to incubate a fatigue crack (N_{Inc}). Following this stage is the microstructurally small crack growth which is the number of cycles in this regime (N_{MSC}). The third stage is the long crack growth that indicates the number of cycles to the failure (N_{LC}). These stages are represented in equation (1) [9] that demonstrates the total number of cycles until failure.

$$N_{Total} = N_{Inc} + N_{MSC} + N_{LC} \tag{1}$$

Crack growth in the microstructurally small crack growth regime is driven by the change of crack tip displacement (ΔCTD). Equation (2) [9], demonstrates this by multiplying the material constant of χ (which reflects crack tip irreversibility) by the difference of crack tip displacement and the crack tip displacement threshold. The crack tip displacement threshold is calculated based on the burgers vector.

$$\left(\frac{da}{dN}\right)_{\text{MSC}} = \chi(\Delta\text{CTD} - \Delta CTD_{th}) \tag{2}$$

As for the other constants, they are better utilized in equation (3) [9]. The C_I and C_{II} are the low cycle and high cycle fatigue constants for small cracks. In the same mathematical model, the *GS* and *GO* represent the grain size with its orientation for the material. GS_0 and GO_0 show the reference grain size and orientation, respectively. $\Delta\hat{\sigma}$ is the equivalent applied stress and *U* is considered as the load ratio parameter. It implies that the crack opening occurs in the tensile part of the cyclic load. Initial crack length is specified by "a" and macroscopic maximum plastic shear

strain amplitude is denoted by $\left(\frac{\Delta\gamma^{p}_{max}}{2}|_{macro}\right)$. The parameters that are material constants include $C_I, C_{II}, \varpi, \xi, \varpi', \xi'$ and ζ.

$$\Delta\text{CTD} = C_{II}\left(\frac{GS}{GS_0}\right)^{\varpi}\left(\frac{GO}{GO_0}\right)^{\xi}\left[\left(\frac{U\Delta\widehat{\sigma}}{S_{ut}}\right)^{\zeta}\right]a + C_I\left(\frac{GS}{GS_0}\right)^{\varpi'}\left(\frac{GO}{GO_0}\right)^{\xi'}\left(\frac{\Delta\gamma^{p}_{max}}{2}|_{macro}\right)^{2} \quad (3)$$

The material constants that were kept the same for each AM process are as listed in Table 2. They were kept within the range of the bounds of the MSF code to avoid any inconsistencies. For example, the crack tip displacement threshold value based on burgers vector for titanium, was set to 3×10^{-9} [9] . The only parameter that was changed for each AM process outside of the small crack stage is strain hardening exponent in the incubation stage [9]. This can only be manipulated when certain information was not given for the small crack stage. Cyclic strain hardening exponent from fatigue testing of each of the AM processes was extracted from literature to correct the curve. Most often this parameter affects the slope of the curve for the material. The parameters that are not material constants were then calibrated to fit the curve to the datapoints on the graph. The values for each of these parameters when the curve is fitted to the datapoints will then be compared for each of the AM methods. The differences in these parameters will represent them as dependent on the additive manufacturing process.

Table 2 - Microstructurally small crack calibration constants for the MSF model of Ti-6Al-4V

Material Constant	**Description**	**Value**
C_I	Low cycle fatigue constant	10000
C_{II}	High cycle fatigue constant	2
ϖ	Pore effect coefficient	0.5
γ	Crack growth rate constant	0.32

3- Results and discussion

In the multistage fatigue model, four of the parameters in microstructurally small crack stage were identified as process dependent. All these microstructural parameters are listed in Table 3. The effect of pore size to local plastic strain (POREEXP) parameter is how the size of the pore can influence the curve when increased or decreased. This parameter had a noticeable effect for each additive manufacturing method in where it can greatly shift the curve when calibrated. Another parameter is the final crack size (a_f) which is the length of the crack until it moves to the long crack fatigue stage. This parameter's value is decreased for each additive manufacturing method to be able to move the curve for each method. The exponents for the grain size (DCSEXP) and grain orientation (GOEXP) were used to calibrate to see how those changes would shift or elongate the fatigue curve.

For comparison purposes, fatigue curve of conventional Ti-6Al-4V was also calibrated in this study. Figure 2 presents the calibrated graphs of conventional and all AM methods. For conventional case in Figure 2(a), the POREEXP parameter value needed to be decreased since the datapoints produced from the code were on the left side of the curve. This parameter heavily influenced the number of cycles to the failure of the conventional Ti-6Al-4V, as by decreasing its value, it decreased the number of cycles. As for the final crack size a_f, it only had a small effect on

the low cycle fatigue regime on the curve. These parameters were the only ones calibrated in the microstructurally small crack stage in order to align the curve with datapoints. The calibrated EBM graph has been shown in Figure 2(b). The change in POREEXP parameter in EBM resulted in a different behavior compared to the conventional case, as by increasing the value for this parameter, it decreased the number of cycles. EBM had a larger pore size and PORENND parameter compared to the conventional case which is due to the material being additively manufactured. In addition, the a_f parameter still mainly influenced the low cycle fatigue regime, however, the GOEXP and DCSEXP mainly affected the high cycle fatigue regime by elongating the curve. For the LENS method shown in Figure 2(c), the top portion of the curve was not affected by the change in the final crack size value. But for the POREEXP parameter, increasing its value increased the number of cycles. This same behavior was noticed in Figure 2(d) for the SLM graph. The difference between EBM and LENS/SLM in this matter is that EBM has the largest pore size, while the other additive manufacturing methods have smaller pore sizes that are less than 50 μm in size, as can be seen in Table 1.

It was observed that similar to conventional case, in LENS and SLM methods, the low cycle fatigue regime is not governed by final crack size, while in EBM, a_f affected the low cycle regime significantly. In addition, grain size exponent's effect on high cycle regime of SLM was more pronounced. It implies that grain size effect can be taken into account in smaller strain amplitudes in SLM which had the finest average grain size.

Table 3 – Process dependent parameters in the multistage fatigue model of Ti-6Al-4V

Parameter	**Conventional**	**EBM**	**LENS**	**SLM**
POREEXP	0.05	2.8	0.35	0.01
a_f	30	50	5	15
GOEXP	0	0.4	0.5	0.7
DCSEXP	0	1	2.5	4

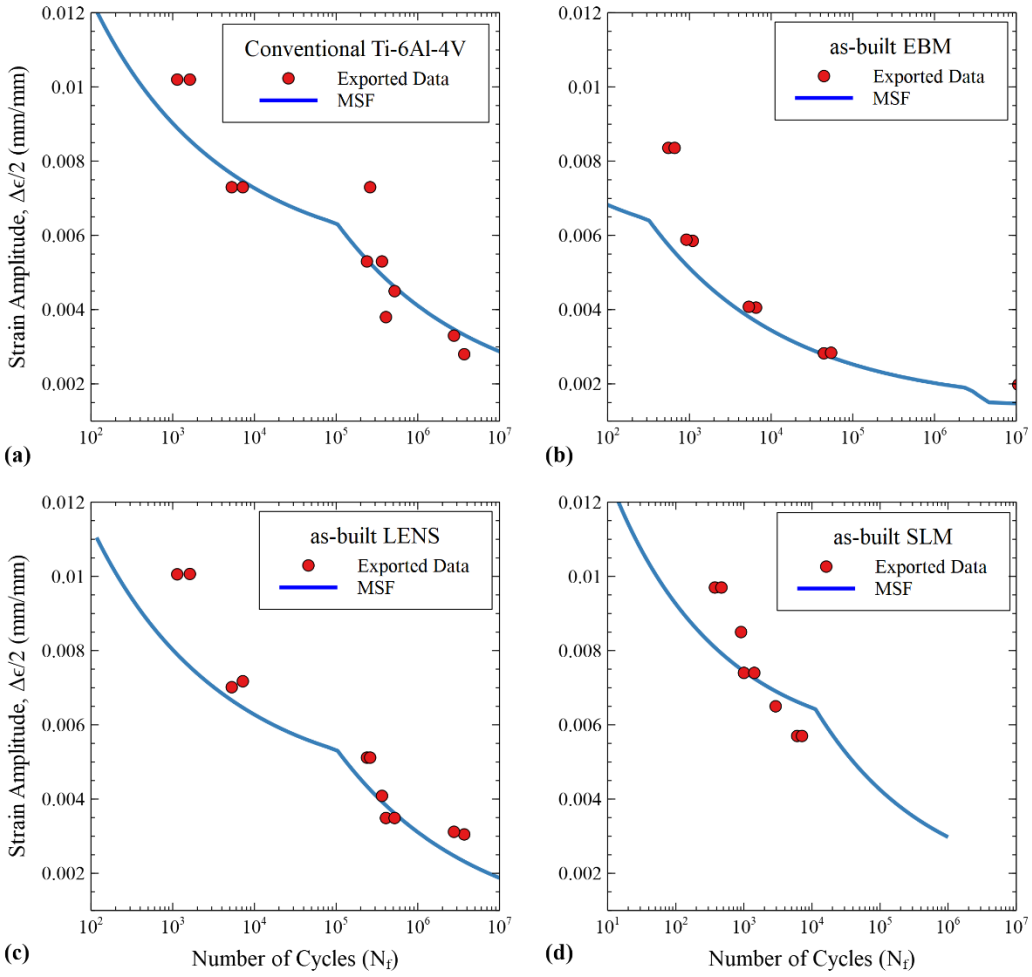

Figure 2- Calibrated fatigue curves using the multistage fatigue model for (a) conventional Ti-6Al-4V, (b) as-built EBM, (c) as-built LENS, and (d) as-built SLM.

4- Conclusions

The multistage fatigue model is used to study the fatigue behavior of Ti-6Al-4V under different additive manufacturing processes. By incorporating microstructural data provided from the scanned electron microscopy, the strain-controlled fatigue curve for each AM method was predicted using MSF model. Results of this study suggest:

1. The fatigue life of specimens was calibrated for Ti-6Al-4V fabricated by conventional, LENS, EBM and SLM methods, just by using data associated with microstructural features and defects such as grain size, pore size and pores distance. Conventional Ti-6Al-4V, showed superior fatigue life compared to additively manufactured cases.
2. Four parameters were identified to be process dependent when comparing the different additive manufacturing processes. These are final crack size, effect of pore size to plastic strain, grain size exponent, and grain orientation exponent in the MSF model.
3. The effects of pore size to local plastic strain parameter were the same for the LENS and SLM. Conversely, when increasing its value for EBM, that decreased the number of cycles. This behavior can be attributed to the large pore size in EBM.

4. In LENS and SLM methods, final crack size did not have influence on low cycle fatigue regime while for EBM, it was governing parameter in that region.
5. The grain size exponent had significant influence on high cycle regime in SLM, indicating its fine grain size affects its fatigue resistance in small strain amplitudes.

References

1. Aboutaleb, A.M., et al., *Multi-objective accelerated process optimization of mechanical properties in laser-based additive manufacturing: Case study on Selective Laser Melting (SLM) Ti-6Al-4V.* Journal of Manufacturing Processes, 2019. **38**: p. 432-444.
2. Sidambe, A.T., *Biocompatibility of Advanced Manufactured Titanium Implants-A Review.* Materials (Basel, Switzerland), 2014. **7**(12): p. 8168-8188.
3. Zhai, Y., H. Galarraga, and D.A. Lados, *Microstructure, static properties, and fatigue crack growth mechanisms in Ti-6Al-4V fabricated by additive manufacturing: LENS and EBM.* Engineering Failure Analysis, 2016. **69**: p. 3-14.
4. Niinomi, M., *Mechanical biocompatibilities of titanium alloys for biomedical applications.* Journal of the Mechanical Behavior of Biomedical Materials, 2008. **1**(1): p. 30-42.
5. Leuders, S., et al., *On the mechanical behaviour of titanium alloy TiAl6V4 manufactured by selective laser melting: Fatigue resistance and crack growth performance.* International Journal of Fatigue, 2013. **48**: p. 300-307.
6. Hrabe, N., T. Gnäupel-Herold, and T. Quinn, *Fatigue properties of a titanium alloy (Ti–6Al–4V) fabricated via electron beam melting (EBM): Effects of internal defects and residual stress.* International Journal of Fatigue, 2017. **94**: p. 202-210.
7. Qiu, C., N.J.E. Adkins, and M.M. Attallah, *Microstructure and tensile properties of selectively laser-melted and of HIPed laser-melted Ti–6Al–4V.* Materials Science and Engineering: A, 2013. **578**: p. 230-239.
8. Liu, S. and Y.C. Shin, *Additive manufacturing of Ti6Al4V alloy: A review.* Materials & Design, 2019. **164**: p. 107552.
9. McDowell, D.L., et al., *Microstructure-based fatigue modeling of cast A356-T6 alloy.* Engineering Fracture Mechanics, 2003. **70**(1): p. 49-80.
10. Zhai, Y., et al., *Fatigue crack growth behavior and microstructural mechanisms in Ti-6Al-4V manufactured by laser engineered net shaping.* International journal of fatigue, 2016. **93**: p. 51-63.
11. Agius, D., K. Kourousis, and C. Wallbrink, *A Review of the As-Built SLM Ti-6Al-4V Mechanical Properties towards Achieving Fatigue Resistant Designs.* Metals (Basel), 2018. **8**(1): p. 75.
12. Rohatgi, A., *Webplotdigitizer: Version 4.5.* 2021.
13. Schneider, C.A., W.S. Rasband, and K.W. Eliceiri, *NIH Image to ImageJ: 25 years of image analysis.* Nature Methods, 2012. **9**(7): p. 671-675.
14. Fatemi, A., et al., *Multiaxial fatigue behavior of wrought and additive manufactured Ti-6Al-4V including surface finish effect.* International journal of fatigue, 2017. **100**: p. 347-366.
15. Sterling, A., et al., *Fatigue Behaviour of Additively Manufactured Ti-6Al-4V.* Procedia engineering, 2015. **133**: p. 576-589.